

Noise-independent Route towards the Genesis of a COMPACT Ansatz for Molecular Energetics: a Dynamic Approach

Dipanjali Halder¹, Dibyendu Mondal¹, Rahul Maitra^{1,2,†}

¹ *Department of Chemistry,*

Indian Institute of Technology Bombay, Powai, Mumbai 400076, India

² *Centre of Excellence in Quantum Information, Computing, Science and Technology,*

Indian Institute of Technology Bombay, Powai, Mumbai 400076, India

[†] *rmaitra@chem.iitb.ac.in*

Recent advances in quantum information and quantum science have inspired the development of various compact dynamic structured ansätze that are expected to be realizable in the Noisy Intermediate-Scale Quantum (NISQ) devices. However, such ansätze construction strategies hitherto developed involve considerable measurements, and thus they deviate significantly in NISQ platform from their ideal structures. Therefore, it is imperative that the usage of quantum resources must be minimized while retaining the expressivity and dynamical structure of the ansatz that can adapt itself depending on the degree of correlation. We propose a novel ansatz construction strategy based on the *ab-initio* many-body perturbation theory that requires *no* pre-circuit measurement and thus it remains structurally unaffected by any hardware noise. The accuracy and quantum complexity associated with the ansatz are solely dictated by a pre-defined perturbative order as desired and hence are tunable. Furthermore, the underlying perturbative structure of the ansatz construction pipeline enables us to decompose any high-rank excitation that appears in higher perturbative orders into the product of various low-rank operators, and it thus keeps the execution gate-depth to its minimum. With a number of challenging applications on strongly correlated systems, we demonstrate that our ansatz performs significantly better, both in terms of accuracy, parameter count and circuit depth, in comparison to the allied unitary coupled cluster based ansätze.

I. INTRODUCTION

Quantum computers have surfaced as a promising computational platform that possesses enormous potential in tackling challenges that are beyond the capabilities of conventional classical computers. Simulation of many-body quantum systems is particularly challenging for classical computers due to the exponential scaling of the computational complexities. Hence, many-body problems pertinent to the field of quantum chemistry, condensed matter physics, and materials science is regarded as a crucial near-term application of the quantum computers and is believed to be among the initial domains to exploit “quantum advantage”¹. Owing to the recent experimental breakthroughs in the realm of quantum technologies, quantum computers have stepped into the noisy intermediate-scale quantum (NISQ) era, in which the quantum hardware are unfortunately not yet capable of attaining fault-tolerant quantum computations. The contemporary state-of-the-art NISQ hardware are known to suffer from short coherence times, limited number of qubits, imprecise readouts and noisy operations, which are the major obstacles towards the practical demonstration of “quantum advantage”. In order to alleviate the limitations of the imperfect NISQ hardware, the preceding decade has witnessed the emergence of hybrid quantum-classical algorithms, viz. variational quantum algorithms (VQAs). The first VQA, namely variational quantum eigensolver (VQE)² was proposed by Peruzzo and co-workers in 2014 to address the electronic structure problem, i.e., to solve for the ground state of

the many-electron Schrodinger equation. The algorithm was first experimentally realized on a photonic quantum computer², followed by its successful demonstrations on superconducting³ and trapped ion quantum hardware^{4,5}. VQE, which is built upon the fundamental concept of variational principle can be realized as a general framework that aims to find the best variational approximation to the ground state energy of a given Hamiltonian through an iterative minimization of energy expectation value with a trial wavefunction ansatz, encoded via a parametrized quantum circuit. VQE relies on both quantum resources, quantified by circuit complexities associated with the parametrized ansatz and classical resources, quantified by the speed at which the minimization process converges. This distinct hybrid nature of VQE primarily accounts for its compatibility with the current pre fault-tolerant NISQ hardware. However, the feasibility of its implementation relies on the circuit complexities of the ansatz. An ansatz not only dictates the feasibility of implementation of VQE, it also significantly impacts the accuracy of estimated energies and optimization landscapes⁶. Hence, it is imperative to tailor an ansatz that balances the trade-offs between accuracies and circuit complexities. Over the last few years, there have been varied developments in pursuit of this goal, with the chemically motivated unitary coupled cluster (UCC)^{2,7} ansatz being the first one to be introduced and studied in the framework of VQE. Although UCC theory was originally proposed decades back, it recently experienced a massive resurgence of interest post its appearance in the seminal work of Peruzzo *et al*². UCC truncated at singles and doubles excitation level (UCCSD) is often considered as a ubiquitous

choice for compact representation of many-electron wavefunction. However, UCCSD turns out to be not expressive enough, especially in the regions of molecular strong correlation. Drawing inspirations from Nakatsuji’s density theorem⁸ and Nooijen’s conjecture⁹, one may improve the expressibility of UCCSD framework by replacing the usual rank-one and rank-two hole-particle excitations by the generalized rank-one and generalized rank-two operators, respectively. While this is expected to recover most of the missing correlation of UCCSD, it also comes with tremendous computational overhead. A recent study carried out by Lee and co-workers have focused on retaining only paired generalized double “excitations”, giving rise to the k-UpCCGSD¹⁰ ansatz for which the circuit depth theoretically scales linearly. With a similar motivation, few of the present authors have introduced a unitarized dual exponential coupled cluster based ansatz, viz., UiCCSDn¹¹, which is capable of simulating the high-rank correlation effects employing rank-one and rank-two parametrization via nested commutators between usual rank-two cluster operators and rank-two vacuum-annihilating scattering operators. Aiming towards further compactification of the ansatz for NISQ realization, Grimsley *et. al.*¹² introduced a dynamically structured ansatz, namely ADAPT-VQE that iteratively selects the “best” set of operators through energy gradient evaluation. Although, ADAPT-VQE is capable of extracting the correlation energy employing a very small subset of operators, the operator selection procedure itself incurs a very high measurement overhead. Following the advent of ADAPT-VQE, there has been numerous studies focusing on the ways to minimize the measurement overhead associated with the operator selection protocol. To this end, the present authors have proposed a dynamic ansatz construction recipe, COMPASS¹³, which employs the energy sorting and operator commutativity prescreening criteria to span the N -electron Hilbert space at bare minimum circuit complexities and measurement overhead. In an attempt to minimize the quantum complexities associated with VQE, Metcalf *et. al.* introduced the double unitary coupled cluster (DUCC)^{14,15} method to downfold the correlation effects into an active space of reduced dimensionality, leading to a resource efficient approach. In 2022, Fedorov and co-workers came up with the unitary selective coupled cluster (USCC)¹⁶ approach inspired by the fundamental ideas of selective heat-bath configuration interaction (SHCI). USCC employs the electronic Hamiltonian matrix elements and amplitudes for excitation operators to determine the “important” excitations to tailor the optimal ansatz. Very recently, Haider *et. al.*¹⁷ introduced compactification of trotterized UCCSDT ansatz via restricting the operators by spin and orbital symmetries. Fan *et. al.*¹⁸ proposed an energy sorting procedure for operator screening within the UCC framework towards the development of a compact and resource efficient ansatz.

The various static structured ansätze like UCCSD or UCCSDT include several operators which are not significant or physically meaningful; however, their inclusion leads to a pronounced proliferation of gate depth. Thus NISQ devices prefer expressive yet compact ansatz with minimal number of relevant parameters that may be selected dynamically depending on the system under consideration. However, most of the dynamic methods hitherto developed require substantial pre-circuit measurements to construct the unitary which add significantly to computation overhead. More importantly, such a dynamic construction of the ansatz (ADAPT-VQE or COMPASS) was proposed based on an ideal quantum environment. However, in the present noisy quantum architecture, a measurement based dynamic circuit tailoring protocol may need to undergo a paradigm shift in the way the operators are selected from the pool as the unitary generated in NISQ hardware is often far from being optimal. Thus, one must minimize the usage of quantum resources for such dynamic ansatz construction, and instead, should rely more on first-principle based or intuitive approaches that may navigate past any potential pitfall posed by the NISQ architecture¹⁹. This paves the motivation to this development: we, for the first time, develop a first-principle based strategy starting from many-body perturbation theory (MBPT)^{20,21} that dynamically constructs an extremely compact yet highly expressive ansatz *without any pre-circuit measurement*. At this stage, one should note that it is the *ansatz construction pipeline* that is measurement-free; however, the iterative optimization of the ansatz parameters would still require measurements. We term such an ansatz construction protocol as Cognitive Optimization via Many-body Perturbation theory towards Ansatz Construction and Tailoring (COMPACT).

In the following section, we first briefly discuss the preliminaries of VQE which also concisely introduces the approach we are going to adopt. The generation of the COMPACT dynamic ansatz pivoted upon the MBPT will subsequently be expounded in an order-by-order manner in Sec. II B. In Section III, we will discuss the general implementation strategy, followed by an in-depth analysis of the performance of COMPACT in determining the ground state energies of a few strongly correlated molecules. Finally, in Section IV, we would summarize our findings along with introducing a roadmap towards possible further developments.

II. THEORY

A. Preliminaries on Variational Quantum Eigensolver (VQE) algorithm and the motivation towards the development of MBPT guided ansatz:

Within this section, we aim to explicate the key fundamentals of the VQE algorithm. We begin by revisiting what lies at the very core of VQE i.e., the variational principle, which states that the exact ground state energy of a system is the global minima of the expectation value of the system Hamiltonian. In mathematical terms, variational principle can be expressed as follows:

$$E_0 \leq \min_{\Phi} \langle \Phi | H | \Phi \rangle \quad (1)$$

Here E_0 denotes the true ground state energy of a molecular system of interest, Φ represents a normalized trial wave function and H denotes the electronic Hamiltonian of the concerned molecular system, whose representation in the language of second quantized operators is given as:

$$H = \sum_{pq} h_{pq} a_p^\dagger a_q + \frac{1}{4} \sum_{pqrs} h_{pqrs} a_p^\dagger a_q^\dagger a_s a_r. \quad (2)$$

where h_{pq} and h_{pqrs} correspond to one- and two-electron integrals respectively, with p, q, r, s indicating general spinorbital indices.

VQE leverages the fundamental concept of the variational principle to obtain an upper bound estimate for the elusive ground state energy of a many-electron system. Its essence lies in the meticulous selection of the initial ‘‘guess’’ for the target ground state wavefunction, commonly referred to as the trial wavefunction ansatz. On a quantum hardware, an ansatz is realized via a parametrized quantum circuit, encompassing a series of parametrized unitary operations. In order to approximate the true ground state energy, VQE intends to search for the optimal set of parameters, i.e., the parameters which lead to minimization of the expectation value of the Hamiltonian. This is achieved via a classical optimizer, which adjusts the parameters of the ansatz iteratively, till the energy expectation value converges to a minimum. A succinct mathematical representation of the overall VQE algorithm is given by

$$E_0 = \min_{\vec{\theta}} \langle \Phi_{HF} | U^\dagger(\vec{\theta}) H U(\vec{\theta}) | \Phi_{HF} \rangle \quad (3)$$

where, $|\Phi_{HF}\rangle$ refers to the Hartree-Fock reference determinant which is commonly used to represent the closed shell many-electron wavefunction, $U(\vec{\theta})$ refers to the series of parameterized unitary operations and $\vec{\theta}$ refers to the set of variational parameters.

A salient feature of VQE is its hybrid nature, making it amenable to the near term noisy quantum devices, albeit the degree of feasibility depends on the choice of the ansatz to a great extent. Expectedly, a shallow depth ansatz would enhance the amenability for

NISQ realization and vice versa. Hence, an ansatz is considered to be the prime ingredient toward the successful implementation of VQE. A succinct overview of all the noteworthy ansätze in the context of VQE have been well documented in ^{6,7}. In this section we restrict ourselves to a fundamental chemistry inspired unitary coupled cluster ansatz (UCC), as it acts as the cornerstone towards COMPACT.

The UCC ansatz employs an exponential operator, where the exponent is taken to be an anti-hermitian sum of hole-particle excitation and de-excitation operators

$$|\Phi_{UCC}\rangle = e^{T(\theta) - T^\dagger(\theta)} |\Phi_{HF}\rangle \quad (4)$$

$$= e^{\tau(\theta)} |\Phi_{HF}\rangle \quad (5)$$

where the cluster operator T is defined as: $T = T_1 + T_2 + T_3 + \dots$. The excitation operator T_n generates the n -th excited determinants from the Hartree-Fock reference.

$$T_1 |\Phi_{HF}\rangle = \sum_{i;a} \theta_i^a |\Phi_i^a\rangle \quad (6)$$

$$T_2 |\Phi_{HF}\rangle = \sum_{i,j;a,b} \theta_{ij}^{ab} |\Phi_{ij}^{ab}\rangle \quad (7)$$

⋮

where the indices i, j refer to occupied spinorbitals and a, b refer to unoccupied spinorbitals with respect to the Hartree Fock reference. The amplitudes θ_i^a and θ_{ij}^{ab} refer to the cluster amplitudes which act as the variational parameters. It is a common practice to restrict the rank of T to be two-body resulting in UCCSD. UCCSD is known to have limited expressibility, thereby suffers from restricted applicability for strong correlation.

One of the first approaches towards the compactification of the UCCSD ansatz was proposed by Romero²² who restricted the number of cluster operators that enters in Trotterized UCCSD by screening them through their first order perturbative values. The authors had demonstrated that such a restriction on the parameters results in drastic compactification of the ansatz without unduly sacrificing the characteristic accuracy of the parent UCCSD. One may think of its higher order generalizations and selectively include (explicitly or implicitly) the *important* rank-three, four,... cluster operators by screening them from their respective leading perturbative order. Our endeavor is a step towards such an intuitive construction of the dynamic ansatz which is intimately guided by many-body perturbation theory. Furthermore, we will decompose any such high rank excitation terms through commutators of certain low rank operators in an optimal way such that the circuit depth remains at its minimum. Such a dynamic construction requires *no* quantum measurements, safeguarding it against any uncertainty that a measurement-based construction of a dynamic ansatz ought to suffer in the NISQ devices.

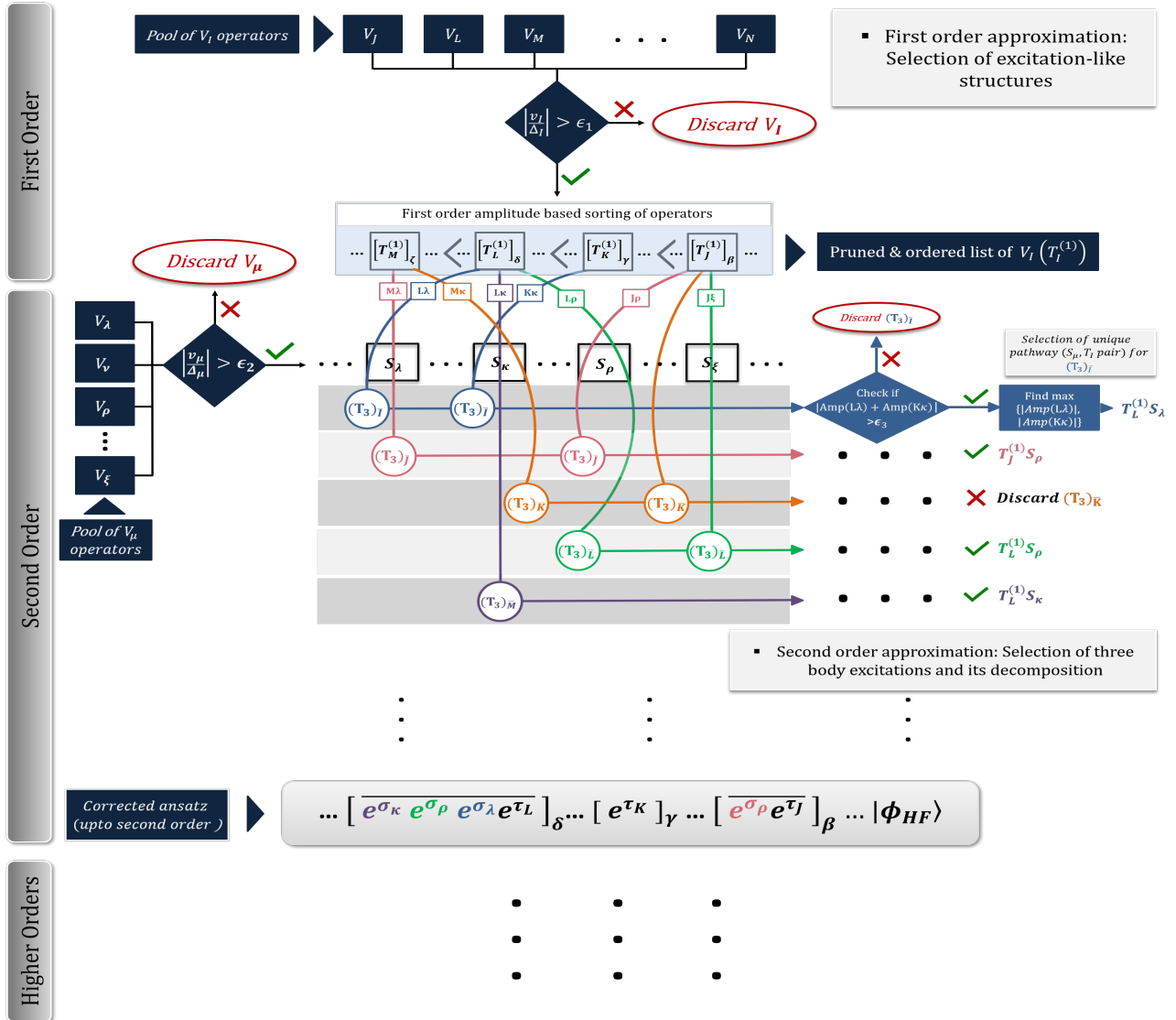


FIG. 1. The hierarchical structure of the COMPACT ansatz construction pipeline at various perturbative orders. The curved lines connecting the various T_I 's (generated at the first order) to some selected S_μ 's are based on the commonality of the contractible indices and such a path leading to the generation of triples are generically denoted as $(I\mu)$. For each T_3 , all such contributions from various paths are summed over to check if the resultant is greater than a threshold ϵ_3 and only the most dominant contributing path is retained. The generation of singles is not shown for brevity. The procedure is repeated for generating higher order terms.

B. Operators selection and ansatz construction pipeline towards COMPACT:

For UCCSD ansatz, a common practice is to initialize the doubles amplitudes from their first order perturbed values that contribute to the MP2 energy. In most of the closed shell applications, the Fock operator is often chosen as the unperturbed Hamiltonian while the perturbation V is taken to be the difference between the electron-electron Coulomb interaction and the Hartree-

Fock potential.

$$V = \sum_i^N \sum_{j>i}^N \frac{1}{|\vec{r}_i - \vec{r}_j|} - \sum_i^N v_{HF}(i) \quad (8)$$

A perturbative expansion of the wavefunction in terms of V thus gives us a recipe to decipher which set of operators first appear at various perturbative orders. This leads one to suitably approximate and filter various rank of excitations based on the respective lowest orders in which they appear to tailor an ansatz. In the following, motivated by MBPT, we take a bottom-up approach

where we hierarchically move upwards the perturbation ladder to select the most important excitations and dynamically construct the ansatz.

1. First-order perturbative correction to the wavefunction: Selection of the double excitation manifold

The selection of the two-body operators based on their first order estimates is well studied and has been previously employed to reduce the parameter space²². While this is well-understood and obvious, we still briefly discuss this formally from the perturbation theoretic standpoint such that we maintain continuity in the next section.

With the choice of the Hartree-Fock determinant $|\Phi_{HF}\rangle$ taken to be the unperturbed function $|\Psi_0^{(0)}\rangle$, the first order correction to the ground state wavefunction may be expressed in terms of $|\Psi_n^{(0)}\rangle$, the zeroth order eigenfunctions of the Fock operator:

$$|\Psi_0^{(1)}\rangle = \sum_{n \neq 0} \left[\frac{\langle \Psi_n^{(0)} | V | \Psi_0^{(0)} \rangle}{E_0^{(0)} - E_n^{(0)}} \right] |\Psi_n^{(0)}\rangle \quad (9)$$

$$= \sum_{n \neq 0} \left[\frac{V_{n0}}{\Delta E_{0n}^{(0)}} \right] |\Psi_n^{(0)}\rangle \quad (10)$$

One may note that $|\Psi_n^{(0)}\rangle$ are orthogonal to $|\Psi_0^{(0)}\rangle$. Since the perturbation V is two-body, the underlying Slater rule ensures that $|\Psi_n^{(0)}\rangle$ s are only the determinants that span the double excitation manifold. Without further elaboration, Eq. 10 may be written in terms of the many-body basis as:

$$|\Psi_0^{(1)}\rangle = \frac{1}{4} \sum_{ijab} \frac{v_{ij}^{ab}}{\Delta_{ij}^{ab}} |\Phi_{ij}^{ab}\rangle = \frac{1}{4} \sum_I \frac{v_I}{\Delta_I} |\Phi_I\rangle \quad (11)$$

Here the index I is the four orbital index tuple $(abij)$.

Since the double excitations T_2 appear first in the leading perturbative order, choosing them at the very first step of our ansatz construction pipeline is logical. However, instead of an impetuous incorporation of the complete pool of T_2 operators, we assess the importance or the effectiveness of each of the T_2 operators to ensure a shallow depth ansatz: only those double excitation operators are retained whose corresponding absolute value of amplitude at the first order perturbative estimate, $t_I^{(1)} = |v_I/\Delta_I| > \epsilon_1$, where ϵ_1 is a suitable user-defined threshold and the rest are discarded. With N_D number of such operators being screened, we align them in descending order of their absolute values of first order perturbative estimates and place them one by one in an ordered set of operator blocks. These operator ‘‘blocks’’ may be defined as snippets of the final ansatz, each of which starts with one cluster operator selected at the first order. In what follows, some of these individual blocks will be subsequently expanded via second and higher order screening to induce specific higher

rank excitations when acted upon the reference function. Towards this, to begin with N_D cluster operators with $\dots |t_J^{(1)}\rangle > \dots > |t_K^{(1)}\rangle > \dots > |t_L^{(1)}\rangle$, e^{τ_J} is placed in an operator block β, \dots, e^{τ_K} in operator block γ, \dots and so on in a disentangled manner with the operator blocks arranged as $\dots \delta > \dots > \gamma > \dots > \beta > \dots > 1$. More explicitly, the operator strings in operator block β act before those in γ and so on. Thus the unitary constructed through the inclusion of the selected operators at the first MBPT order may be expressed as:

$$U^{[1]} = \dots \left[e^{\tau_L} \right]_{\delta} \dots \left[e^{\tau_K} \right]_{\gamma} \dots \left[e^{\tau_J} \right]_{\beta} \dots$$

$$U^{[1]} = \prod_{\alpha=1}^{N_D} \left[e^{\tau_I} \right]_{\alpha} \quad (12)$$

Here the indices J, K, L are the four orbital index tuple associated with the selected T_2 operators and $\tau = T - T^\dagger = \theta \hat{\kappa}$ is the anti-hermitian operator where $\hat{\kappa}$ is the operator string and θ is the parameter. One may note that such a restriction on the magnitude of the first order estimate of the two-body cluster amplitudes screens out any symmetry-disallowed excitations and thus no additional pruning needs to be performed on top.

2. Second-order perturbative correction to the wavefunction: Selection of the single and triple excitation manifolds

The second order correction to the ground state wavefunction is given by:

$$|\Psi_0^{(2)}\rangle = \sum_{n \neq 0} \left[\sum_{m \neq 0} \frac{\langle \Psi_n^{(0)} | V | \Psi_m^{(0)} \rangle \langle \Psi_m^{(0)} | V | \Psi_0^{(0)} \rangle}{(E_0^{(0)} - E_n^{(0)})(E_0^{(0)} - E_m^{(0)})} - \frac{\langle \Psi_0^{(0)} | V | \Psi_0^{(0)} \rangle \langle \Psi_n^{(0)} | V | \Psi_0^{(0)} \rangle}{(E_0^{(0)} - E_n^{(0)})^2} \right] |\Psi_n^{(0)}\rangle \quad (13)$$

$$= \sum_{n \neq 0} \left[\sum_{m \neq 0} \frac{V_{nm} V_{m0}}{\Delta E_{0n}^{(0)} \Delta E_{0m}^{(0)}} - \frac{V_{00} V_{n0}}{(\Delta E_{0n}^{(0)})^2} \right] |\Psi_n^{(0)}\rangle \quad (14)$$

Clearly, with V taken to be the two-body operator, $|\Psi_m^{(0)}\rangle$ can span the orthogonal doubly excited space while $|\Psi_n^{(0)}\rangle$ are the determinants that span single, double and triple excitation manifold. Note that the doubles are already selected in our ansatz through first order MBPT screening and no more alteration to the two-body excitation operator pool will be done. We will not account for the second term of Eq. 14 as such unlinked terms do not explicitly appear at the second order when the Hamiltonian is taken to be normal ordered with respect to the Hartree-Fock reference²¹. From this second order analysis, we concentrate to select only the dominant single and triple excitation operators which appear for the first time in the perturbative expansion.

Taking $|\Psi_n^{(0)}\rangle$ to be the triply excited determinants, we first prune the three-body excitation manifold depending on the orbital indices. The determinant $|\Psi_n^{(0)}\rangle$ is generated by the *connected* action of the perturbation operator V on the doubly excited determinants $|\Psi_m^{(0)}\rangle$; thus there must be one orbital label (either hole or particle) common between the two perturbation operators V (one that connects $|\Psi_m^{(0)}\rangle$ and $|\Psi_0^{(0)}\rangle$ and the other that connects $|\Psi_m^{(0)}\rangle$ and $|\Psi_n^{(0)}\rangle$). This common orbital label may be considered to be a contractible orbital index. In what follows, among the six orbital indices (3 holes and 3 particles) that characterize each of the triply excited determinants, a set of three orbital tuple (either $2h1p$ or $2p1h$) comes from each V . An expansion of Eq. (14) in the many-body basis would make this evident.

$$|\Psi_0^{(2)}\rangle \leftarrow \sum_{ijkabc} \left[\sum_m \frac{v_{ij}^{am} v_{mk}^{bc}}{\Delta_{ijk}^{abc} \Delta_{mk}^{bc}} + \sum_e \frac{v_{ie}^{ab} v_{jk}^{ec}}{\Delta_{ijk}^{abc} \Delta_{jk}^{ec}} \right] |\Phi_{ijk}^{abc}\rangle \quad (15)$$

which together can be compactly written as:

$$T_{\overline{K}} \leftarrow \frac{\overline{(V_\mu V_I)}_{\overline{K}}}{\Delta_{\overline{K}} \Delta_I} = \frac{\overline{(V_\mu T_I^{(1)})}_{\overline{K}}}{\Delta_{\overline{K}}} \quad (16)$$

where \overline{K} stands for the six orbital index tuple associated with the triple excitation, and μ, I have similar meaning for two-body operators of various structures. The overbarred capitalized indices will generically denote three body excitation structure. Note that the four orbital tuple that characterize the V which connects $|\Psi_m^{(0)}\rangle$ and $|\Psi_n^{(0)}\rangle$ is denoted by Greek letter μ to distinguish it from an excitation-like structure of V_I . To select and parametrize the corresponding triple excitations, we use the following screening criteria:

- **Orbital index based excitation subspace pruning:** With the selected N_D elements at the first order, we generate a set of all unique three-orbital tuples by grouping all the 2-hole and 1-particle or 2-particle and 1-hole orbitals from the list of screened $T_2^{(1)}$. Thus the maximum number of tuple elements in the set is $4N_D$, but in practice this number is significantly less. From Eq. 15, note that any important rank-three operators that lead to three-body excited determinants must contain three orbital indices coming from $T_2^{(1)}$, we thus target to retain only those rank-three operators that have at least one of those unique three-orbital tuples. This significantly compactifies the search space for the selection of the dominant T_3 .
- **Excitation pathway pruning through leading order approximation of the scatterers:** In the classical computer, to have the minimal computational overhead towards the generation and assessment of the important triple excitations, we retain

only those V_μ in the summation in Eq. (16) for which $|v_\mu/\Delta_\mu| > \epsilon_2$, where ϵ_2 is another user defined threshold. It is important to note that the structure of V_μ is that of a two-body operator with effective hole-particle excitation rank of one. The contractible operators (either hole (m) or particle type (e)) in Eq. 15 appear as a *destruction* operator. As such one may introduce a *scatterer operator* S with identical hole-particle structure as V_μ whose leading order measure will be $s_\mu^{(1)} = |v_\mu/\Delta_\mu|$. Here Δ_μ is a local denominator that we had approximated to define the scatterer instead of the global denominator $\Delta_{\overline{K}}$ that appears in Eq. (16). The anti-hermitian operator $\sigma = \theta \hat{\kappa}$ will be used to denote $S - S^\dagger$.

- **Excitation subspace pruning based on the overall contribution:** Finally, with the two criteria above satisfied, we ensure that:

$$\left| \text{Amp} \left(\frac{\overline{(V_\mu T_I^{(1)})}_{\overline{K}}}{\Delta_{\overline{K}}} \right) \right| > \epsilon_3 \quad (17)$$

Here *Amp* suggests the amplitudes part of the corresponding equation. Even though the first two criteria above are satisfied, this criterion ensures that only the most dominant resultant triples are finally included after cancellation of terms with opposite signs. One must note that with the first two criteria (along with the filtering of the two-body amplitudes at first order) above satisfied, the generation of a term like $\overline{(V_\mu T_I^{(1)})}_{\overline{K}}$ requires only a few scalar multiplications and we will exploit this while choosing a dominant unique pathway (*vide infra*).

While one may explicitly include all the selected three-body cluster operators in the UCC ansatz, this leads to a pronounced escalation in the gate count and gate depth. Thus in order to keep the gate depth at its minimum, we decompose every selected T_3 as $T_{\overline{K}} \leftarrow \overline{(S_\mu T_I)}_{\overline{K}}$ as they appear in the second order expansion of the wavefunction Eq. (14)-(16). In the unitarized version, it is straightforward to see that every such contraction between the operators can be captured by a commutator of the associated anti-hermitian operators:

$$[\hat{\kappa}_\mu, \hat{\kappa}_I] \longrightarrow \hat{\kappa}_{\overline{K}} \quad (18)$$

Note that it is important to identify the appropriate operator label μ such that the scatterer $\hat{\kappa}_\mu$ does not commute with the excitation operators $\hat{\kappa}_I$. This means that the contractible destruction operator in S must be common to one of the creation orbital indices in T . To simulate such a high rank excitation, clearly one needs to pair up appropriate τ and σ in a factorized²³ manner such that

$$e^\sigma e^\tau = e^{(\sigma+\tau) + \frac{1}{2}[\sigma, \tau] + \dots} \quad (19)$$

At this stage it is important to note that for a *canonical Hartree-Fock* reference, the triple excitation that appears

in the leading order is represented by explicitly connected diagrams²⁴ as shown in Eq. 16. Thus unlike the work by Fedorov *et. al.*¹⁶ who approximate the triples as disconnected product of two operators, our representation is manifestly connected.

Selection of a unique pathway to triple and higher rank excitation manifold: While the decomposition of the high rank excitation in terms of lower rank operators is attractive, this may often lead to redundant generation of a given triple excitation at the cost of more number of parameters. There may be several pairs of $\hat{\kappa}_\mu$ and $\hat{\kappa}_I$ which leads to the same three-body excitation:

$$[\hat{\kappa}_{\mu_1}, \hat{\kappa}_{I_1}] \longrightarrow \hat{\kappa}_{\overline{K}}$$

$$[\hat{\kappa}_{\mu_2}, \hat{\kappa}_{I_2}] \longrightarrow \hat{\kappa}_{\overline{K}} \quad \text{and so on...}$$

One may expand the implied sum in Eq. (17) into sum of the associated scalar products between the selected V_μ and T_I :

$$\begin{aligned} \text{Amp} \left(\frac{(V_\mu T_I^{(1)})_{\overline{K}}}{\Delta_{\overline{K}}} \right) &= \text{Amp} \left(\frac{(V_{\mu_1} \cdot T_{I_1}^{(1)})_{\overline{K}}}{\Delta_{\overline{K}}} \right) \\ &+ \text{Amp} \left(\frac{(V_{\mu_2} \cdot T_{I_2}^{(1)})_{\overline{K}}}{\Delta_{\overline{K}}} \right) + \dots \end{aligned} \quad (20)$$

and retain only that unique pair of σ_μ and τ_I at the second order for which the absolute value of individual scalar products appearing on the right side of Eq. (20) is maximum. Of course, the corresponding τ_I , which is already included at the first order but whose corresponding $[\sigma, \tau]$ pathway gets excluded at the second order through the unique pathway selection for triples, is not removed from the operator block since the corresponding doubles are important; we simply do not pair up any σ along with it.

With the knowledge of the first order corrected ansatz (Eq. (12)) along with the important triples and the scatterers through the second order screening criteria stated above, we expand the various operator blocks in the ansatz with the second order estimate as:

$$U^{[2]} = \dots \left[\overline{e^{\sigma_{\nu'}} \dots e^{\sigma_\nu} e^{\tau_L}} \right]_\delta \dots \left[e^{\tau_K} \right]_\gamma \dots \left[\overline{e^{\sigma_\lambda} e^{\tau_J}} \right]_\beta \dots \quad (21)$$

One may note that there may be more than one σ that can couple with a given τ to generate two or more distinct three-body terms, all of which may get selected as per the criteria stated before. Thus one operator block may contain more than one σ as shown above; however, there cannot be more than one τ in any given operator block. Furthermore, cases may arise where no σ is chosen through the selection criteria to pair up with a τ to generate triples, as shown in the operator block γ as an example. In general,

$$U^{[2]} = \prod_{\alpha=1}^{N_D} \left[\overline{e^{\sigma_{\mu'}} \dots e^{\sigma_\mu} e^{\tau_I}} \right]_\alpha \quad (22)$$

where the overbars denote the implied commonality of the contractible index between the τ and σ . There may be fortuitous scenario due to the factorized structure of the unitary for which the arrangement of the operators simulates the third order effects of quadruple excitations. For example, in Eq. 21, $e^{\sigma_{\nu'}}$ may act on the composite $e^{\sigma_\nu} e^{\tau_L}$ that simulates a quadruple, whereas both $e^{\sigma_\nu} e^{\tau_L}$ and $e^{\sigma_{\nu'}} e^{\tau_L}$ simulate two distinct triples.

Along with the triples, the singles also are generated for the first time at the second order of MBPT. The selection procedure of the singles at the second order also closely follows the way significant triples are selected. We choose only those singles for which

$$\left| \text{Amp} \left(\frac{(V_{\overline{\mu}} T_I^{(1)})_{\underline{K}}}{\Delta_{\underline{K}}} \right) \right| > \epsilon_3 \quad (23)$$

Note that underbarred and capitalized letters, \underline{K} here represents the tuple of one hole and one particle index and $V_{\overline{\mu}}$ in Eq. (23) are two-body operators with effective $1p-1h$ de-excitation structure. Unlike in Eq. (17), no filtering for V_μ is employed here although the associated $T_I^{(1)}$ s are those which are previously selected at first order. Since T_I s are very few in number and contribute insignificantly to the gate depth, the selected T_I s are parametrized as they are. Note that both in Eqs. (17) and (23), we have usually employed the same threshold since both singles and triples are first generated at the same order. Once the singles are screened, they are appended at the end of Eq. (22) and the final ansatz at the end of second order can be expressed as:

$$U^{[2]} = \prod_{\beta=1}^{N_S} \left[e^{\tau_L} \right]_\beta \prod_{\alpha=1}^{N_D} \left[\overline{e^{\sigma_{\mu'}} \dots e^{\sigma_\mu} e^{\tau_I}} \right]_\alpha \quad (24)$$

where N_S denotes the total number of singles screened.

3. Higher order generalizations

The connected quadruples are generated for the first time in the third order and one may arbitrarily expand the ansatz by including leading order contributions by climbing up the MBPT ladder. Due to the hierarchical structure of the MBPT equations, only the *important* lower order terms may contribute to higher order. Thus with the knowledge of the dominant triples and the dominant σ_ν , exactly the same protocol may be followed while moving to the third order generation of quadruply excited terms as one does while moving from first to second order. The quadruples are thus simulated through the nested commutator: $[\hat{\kappa}_\nu, [\hat{\kappa}_\mu, \hat{\kappa}_I]] \longrightarrow \hat{\kappa}_{K=4}$ where $K=4$ denotes that eight orbital tuple index associated with a given quadruple excitation. Of course, additional care needs to be taken (if one desires so) to include only the unique quadruples that are not fortuitously included at the second order due to the pairing up of more than

one σ to a τ in a given operator block as an artifact of the disentangled structure of the unitary. At this stage, we mention that the third order is the lowest perturbative order where the unlinked diagrams appear and eventually get cancelled by the renormalization terms. Thus our approach towards the construction of the dynamic ansatz satisfies linked cluster theorem and is perturbatively meaningful.

The factorized structure of our ansatz (at any given perturbative order with various unitary operators appearing as a product) bears a resemblance to the disentangled UCC theory (dUCC)²⁵. However, instead of ADAPT-VQE-like gradient based numerical selection and ordering of the operators from a pre-designed operator pool, we base our ansatz construction on perturbative analysis. While at the first order, it leads to the conventional dUCCD ansatz with a specific operator ordering, the higher order many-body perturbative structure naturally incorporate appropriate pair of scattering and cluster operators to be grouped in each operator block to induce high rank excitations via Eqs. 18 and 19.

One may note that the various ranks of cluster operators that are included or implicitly simulated are by construction symmetry adapted, and we do not need to impose additional symmetry constraints. Furthermore, the entire ansatz construction pipeline does not involve any measurement and is solely based on first-principle based perturbation theoretic measures. Due to no measurement overhead involved in COMPACT, the optimal structure of the ansatz is independent of any device noise. A bird's-eye-view of the operator selection scheme at various perturbative order is shown in Fig. 1. Below, we demonstrate the efficacy of the ansatz in capturing electronic strong correlation for various challenging cases.

III. NUMERICAL RESULTS AND DISCUSSIONS

A. Methodology and general considerations

In this section we illustrate the efficacy of our method by computing the ground state potential energy curves for three prototypical molecular systems: LiH , BH and symmetric bond stretching of H_2O . For the numerical simulations, we have employed Qiskit nature²⁶ along with the PySCF module²⁷. For all the calculations we have employed the contracted STO-3G basis²⁸. We have chosen the Jordan-Wigner²⁹ mapping technique to transform the second-quantized operators into the qubitized quantum circuit. For the optimization part of the VQE algorithm, we have worked with the gradient based LBFGS-B³⁰ optimizer with the initial parameters for two-body operators set to their respective first order perturbative estimates and those corresponding to T_1 are set to zero. As the performance of COMPACT hinges upon the meticulous selection of the thresholds ϵ_1 , ϵ_2 and ϵ_3 , we henceforth denote it as COMPACT(-log ϵ_1 , -log ϵ_2 , -log ϵ_3). In all the cases, the reported parameter count

accounts for the spin-complementary excitations as separate independent variables.

B. Potential energy profile of strongly correlated systems: Accuracy, parameter count and CNOT gate count

We demonstrate the efficacy and accuracy of COMPACT with three prototypical systems, namely the stretching of LiH , BH and the simultaneous symmetric stretching of the bonds of H_2O , all of which exhibit intricate interplay of diverse electronic correlation effects. We first investigate the dissociation potential energy profile for LiH molecule. Within the STO-3G basis set, the LiH molecule is characterized as a 12 qubit (spinorbital) system spanned by 4 electrons. In Fig. 2, we have plotted the energy errors with respect to the classically computed FCI energies (Fig. 2(a)), parameters count (Fig. 2(d)) and two qubit CNOT gates count (Fig. 2(g)) of our method for various $Li-H$ bond lengths ranging between 1Å and 4Å, and compared them against the conventional UCCSD, UCCSDT and sym-UCCSDT¹⁷. UCCSD with a parameter count (CNOT gate count) of 92 (7,520) shows a catastrophic failure for stretched bond lengths (see Fig. 2(a)), hinting towards the poor expressibility of the UCCSD ansatz in the regions of molecular strong correlation. UCCSDT, on the other hand, exhibits remarkable accuracy across the entire spectrum of the potential energy surface, however, at the expense of exceedingly large number of parameters (188) and two qubit CNOT gates (52,064). The sym-UCCSDT ansatz shows significant savings in quantum complexities without compromising the accuracies at the expense of only 58 parameters and 14,304 CNOT gates. Remarkably, the parameters count (CNOT gate count) corresponding to COMPACT(5,5,4) in the best case scenario (for geometries around the equilibrium) and the worst case scenario (for stretched geometries) are 44 (3,580) and 54 (4,480) respectively. It is worth pointing out at this juncture that although there is not significant difference between the sym-UCCSDT and COMPACT(5,5,4) in terms of parameter count, COMPACT shows significant reduction in the number of CNOT gates. With a very conservative choice of thresholds, i.e., $\epsilon_1, \epsilon_2 = 10^{-5}$ and $\epsilon_3 = 10^{-4}$, we get an order of magnitude reduction in gate count compared to sym-UCCSDT and UCCSDT. Such savings in circuit depth can be attributed to the fact that COMPACT encapsulates the effects of higher order excitations via only rank-two and rank-one excitations without explicitly involving the higher order excitations, unlike the other conventional methods. One may note that in the NISQ devices that suffer from various sources of detrimental noise, the reduction in the CNOT gate count (rather than the number of parameters) is more desirable, and COMPACT is a significant stride towards this. Additionally for LiH at a strongly correlated regime (bond length 4Å), we have plotted (Fig. 3) the

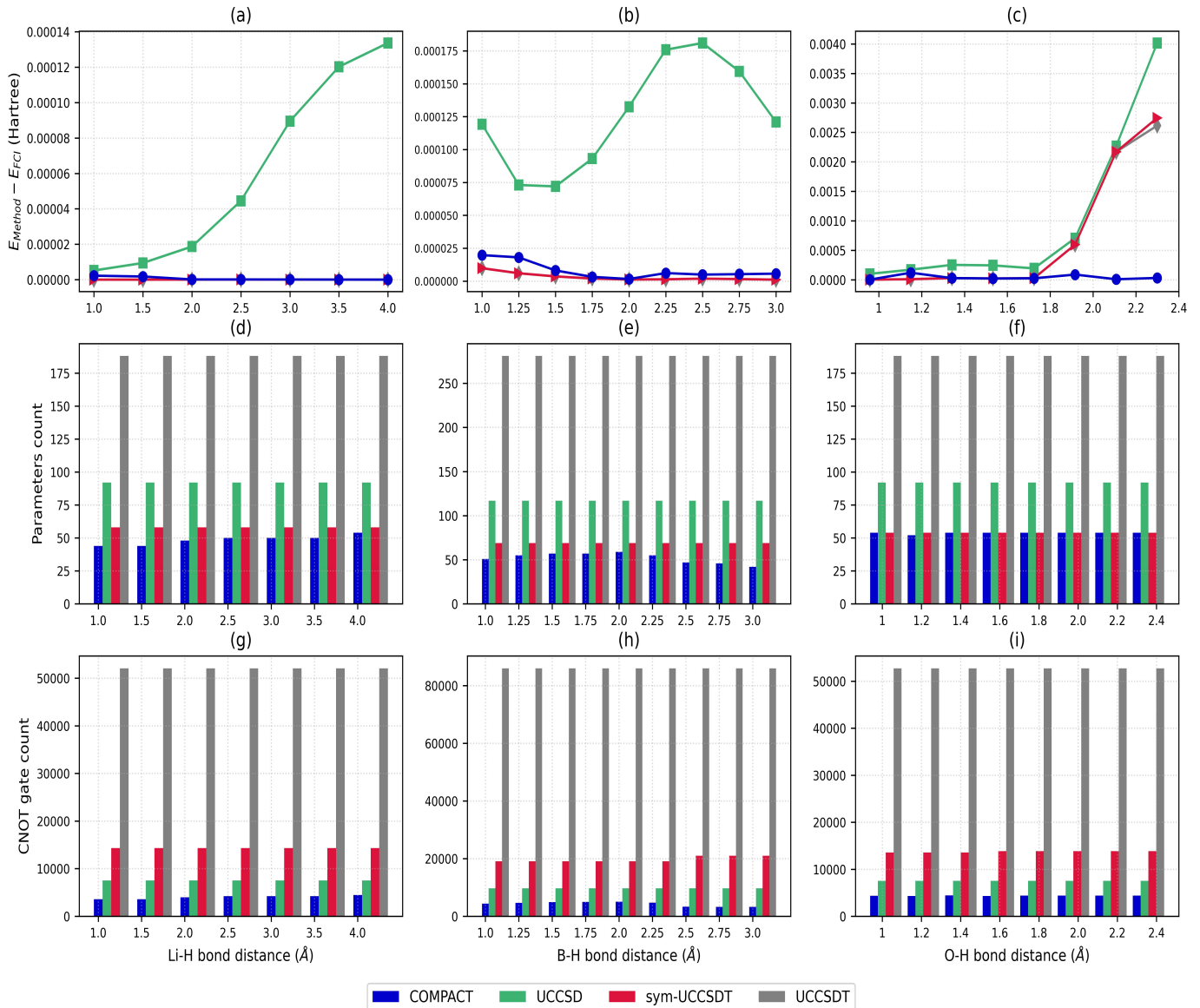


FIG. 2. Energy Error with respect to FCI (first row), parameter count (second row) and execution CNOT gates count per function evaluation (third row) over the potential energy profile for *LiH* (first column), *BH* (second column) and *H₂O* (third column).

overlap of the final state (for UCCSD, sym-UCCSDT and COMPACT) with full configuration interaction (FCI) state and their energy convergence landscape against the number of function evaluations for all these methods. COMPACT clearly demonstrates its superiority over other methods in predicting more accurate states and energy as compared to other methods under choice.

The next system under the consideration is *BH*; the potential energy profile when the *B-H* bond is stretched is challenging to model due to interplay of strong and weak correlation and thus this is considered as a standard testbed for evaluating the performance of a newly developed electronic structure methodology. *BH* in STO-3G basis can be identified as a 6 electron system distributed in 12 qubits (spinorbitals). In Fig. 2(b), we have plotted the energy deviations of COMPACT and other allied con-

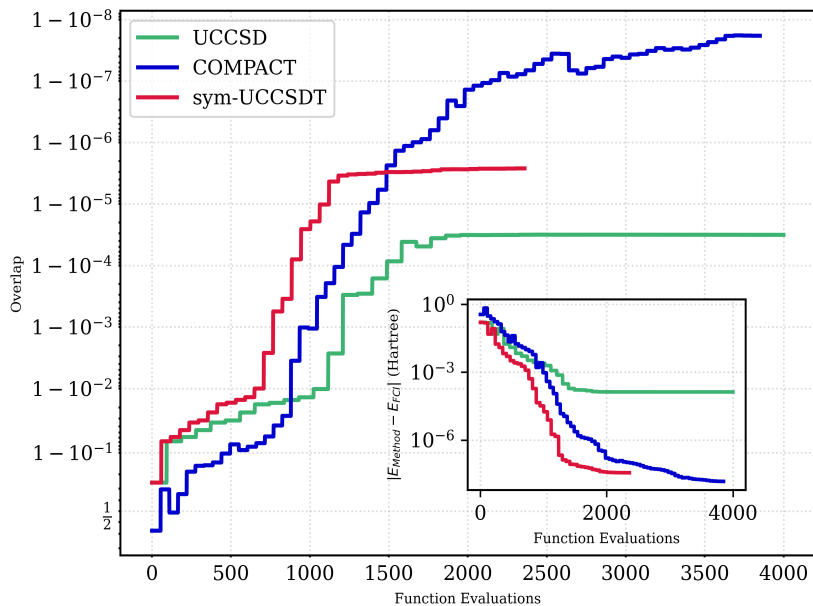


FIG. 3. Convergence trace as measured by the overlap with FCI wavefunction against the number of function evaluations for UCCSD, sym-UCCSDT and COMPACT for LiH at bond length = 4\AA . The inset shows the convergence in predicted energies.

ventional methods (UCCSD, UCCSDT, sym-UCCSDT) with respect to the FCI. While UCCSD exhibits an energy deviation $\sim 10^{-4}$ Hartree for $B-H$ distances beyond 1.75\AA , the same for UCCSDT and sym-UCCSDT is of the order of 10^{-6} Hartree, clearly demonstrating the importance of higher excitations for strongly correlated regions. With the fixed structure of UCCSD, UCCSDT and sym-UCCSDT, their associated parameters count (CNOT gates count) are 117 (9,672), 281 (86,020) and 69 (19,080 for $R_{B-H} < 2.5\text{\AA}$ and 20,976 for $R_{B-H} \geq 2.5\text{\AA}$) respectively. Note that for sym-UCCSDT in STO-3G basis, the change in the virtual orbital symmetries beyond $R_{B-H} = 2.5\text{\AA}$ leads to the change in the number of CNOT count. Interestingly, with thresholds $\epsilon_1, \epsilon_2 = 10^{-3}$ and $\epsilon_3 = 10^{-4}$, COMPACT(3,3,4) follows an energy profile almost as good as UCCSDT and sym-UCCSDT. What is even more alluring, the quantum complexities *i.e.*, parameters count (and the CNOT gates count) corresponding to the COMPACT(3,3,4) ansatz falls within a range: 59 (5,048) (at $R_{B-H} = 2\text{\AA}$) and 42 (3232) (at $R_{B-H} = 3\text{\AA}$), showcasing a tremendous reduction in quantum resources throughout the potential energy profile. The quantum complexities associated with COMPACT and the other conventional ansätze has been illustrated along the various $B-H$ bond lengths in Fig. 2(e) and 2(h).

The final system under consideration is the symmetric simultaneous stretching of $O-H$ bonds in H_2O molecule. With the $1s$ core orbital of O frozen, H_2O in STO-3G basis renders to be a 8 electrons system in 12 spinorbitals. Fig. 2(c) shows the energy accuracy over the potential energy profile ($O-H$ bond lengths ranging

between R_e and 2.4 times R_e with $R_e = 0.958\text{\AA}$ and the $H-O-H$ angle kept fixed at 104.4776°) compared to FCI. Fig. 2(f) and 2(i) showcases a comparative study of the corresponding quantum complexities (parameters count and two qubit CNOT gate count) associated with COMPACT, UCCSD, UCCSDT and sym-UCCSDT. While UCCSD requires 92 (7552) parameters (CNOT gates), it fails catastrophically with the stretching of $O-H$ bonds when the molecular strong correlation kicks in. Unexpectedly, both UCCSDT and sym-UCCSDT too shows similar trend as UCCSD. A possible explanation for such a behaviour might be the inability of both the ansätze in navigating towards the absolute minima. On the other hand, COMPACT (5,5,4) shows remarkable accuracy throughout the potential energy profile at the expense of mere 52-54 parameters and 4308-4440 CNOT gate counts. One may note that the quantum resources deployed by COMPACT is at least one order of magnitude less than those required even by sym-UCCSDT; however, the former ascertainably outperforms the conventional ansätze in terms of accuracy throughout the energy profile. We reiterate that such dramatic reduction in quantum complexity, particularly in the CNOT gate count, makes the realization of COMPACT in NISQ devices seemingly feasible.

Towards the end of this section, we also highlight the scalability of this approach to treat realistic many-body systems. The COMPACT ansatz pre-screen the many-body bases and retains only the “most dominant” terms of the N -electron Hilbert space *at each perturbative order*. These excitations are subsequently included in the construction of COMPACT ansatz via lower rank decom-

position in terms of the cluster operators and a cascade of scatterers. The hierarchical selection of the dominant determinants and the screening at each perturbative order to retain their unique pathway further ensure to restrict the number of parameters and CNOT gate count to their minimum. With the increase in system size, this does not approach the exponential quantum complexity of Full Configuration Interaction as the number of such determinants screened by COMPACT at any given perturbative order practically increases sub-exponentially with the system size.

IV. CONCLUSIONS AND FUTURE OUTLOOK

In this study, we have proposed a novel algorithm towards an intuitive construction of a dynamic structured ansatz in a system-specific manner. COMPACT caters to the dual objective of minimization of circuit depth while concurrently eliminating the necessity of any pre-circuit measurements towards the construction of an optimally expressive ansatz. Unlike most of the prevalent dynamic ansätze, COMPACT relies on classical approximations for ansatz construction and compactification; thus, it is safeguarded from any kind of quantum hardware induced noise. Built upon the many-body perturbation theory, the accuracy and quantum complexities associated with COMPACT are reliant only on the perturbative order and hence, are tunable.

Through a number of numerical applications on prototypical strongly correlated molecular systems, we have demonstrated that the resulting ansatz is expressive enough to handle molecular strong correlation with only a shallow circuit depth and zero measurement overhead in its construction process. While the genesis of the ansatz is performed “classically”, it still requires quantum measurements for the iterative optimization of the parameters and thus the final outcome (but not the structure of the ansatz) is likely to get impacted by hardware noise. In this regard, it would be interesting to introduce CNOT-efficient circuits^{31–33} with additional error mitigation routines³⁴ for COMPACT which is likely to be further resilient to hardware noise during its execution. COMPACT may also be implemented in terms of the Quantum Flow algorithm³⁵ in reduced dimensionality active spaces to further minimise its final circuit complexity. An excited state extension to COMPACT will also be highly desirable and will be a subject of our future endeavors in this direction.

ACKNOWLEDGEMENTS

D.H. thanks the Industrial Research and Consultancy Center (IRCC), IIT Bombay and D.M. acknowledges the Prime Minister’s Research Fellowship (PMRF), Government of India for their research fellowships.

CONFLICT OF INTERESTS

The authors have no conflict of interests to disclose.

DATA AVAILABILITY

The data that support the findings of this study are available from the corresponding author upon reasonable request.

- ¹S. McArdle, S. Endo, A. Aspuru-Guzik, S. C. Benjamin, and X. Yuan, “Quantum computational chemistry,” *Rev. Mod. Phys.* **92**, 015003 (2020).
- ²A. Peruzzo, J. McClean, P. Shadbolt, M.-H. Yung, X.-Q. Zhou, P. J. Love, A. Aspuru-Guzik, and J. L. O’Brien, “A variational eigenvalue solver on a photonic quantum processor,” *Nature Communications* **5** (2014), 10.1038/ncomms5213.
- ³P. J. J. O’Malley, R. Babbush, I. D. Kivlichan, J. Romero, J. R. McClean, R. Barends, J. Kelly, P. Roushan, A. Tranter, N. Ding, B. Campbell, Y. Chen, Z. Chen, B. Chiaro, A. Dunsworth, A. G. Fowler, E. Jeffrey, E. Lucero, A. Megrant, J. Y. Mutus, M. Neeley, C. Neill, C. Quintana, D. Sank, A. Vainsencher, J. Wenner, T. C. White, P. V. Coveney, P. J. Love, H. Neven, A. Aspuru-Guzik, and J. M. Martinis, “Scalable quantum simulation of molecular energies,” *Phys. Rev. X* **6**, 031007 (2016).
- ⁴Y. Shen, X. Zhang, S. Zhang, J.-N. Zhang, M.-H. Yung, and K. Kim, “Quantum implementation of the unitary coupled cluster for simulating molecular electronic structure,” *Phys. Rev. A* **95**, 020501 (2017).
- ⁵C. Hempel, C. Maier, J. Romero, J. McClean, T. Monz, H. Shen, P. Jurcevic, B. P. Lanyon, P. Love, R. Babbush, A. Aspuru-Guzik, R. Blatt, and C. F. Roos, “Quantum chemistry calculations on a trapped-ion quantum simulator,” *Phys. Rev. X* **8**, 031022 (2018).
- ⁶J. Tilly, H. Chen, S. Cao, D. Picozzi, K. Setia, Y. Li, E. Grant, L. Wossnig, I. Rungger, G. H. Booth, and J. Tennyson, “The variational quantum eigensolver: A review of methods and best practices,” *Physics Reports* **986**, 1–128 (2022), the Variational Quantum Eigensolver: a review of methods and best practices.
- ⁷A. Anand, P. Schleich, S. Alperin-Lea, P. W. K. Jensen, S. Sim, M. Díaz-Tinoco, J. S. Kottmann, M. Degroote, A. F. Izmaylov, and A. Aspuru-Guzik, “A quantum computing view on unitary coupled cluster theory,” *Chem. Soc. Rev.* **51**, 1659–1684 (2022).
- ⁸H. Nakatsuji, “Equation for the direct determination of the density matrix,” *Phys. Rev. A* **14**, 41–50 (1976).
- ⁹M. Nooijen, “Can the eigenstates of a many-body hamiltonian be represented exactly using a general two-body cluster expansion?” *Phys. Rev. Lett.* **84**, 2108–2111 (2000).
- ¹⁰J. Lee, W. J. Huggins, M. Head-Gordon, and K. B. Whaley, “Generalized unitary coupled cluster wave functions for quantum computation,” *Journal of Chemical Theory and Computation* **15**, 311–324 (2019), <https://doi.org/10.1021/acs.jctc.8b01004>.
- ¹¹D. Halder, V. S. Prasanna, and R. Maitra, “Dual exponential coupled cluster theory: Unitary adaptation, implementation in the variational quantum eigensolver framework and pilot applications,” *The Journal of Chemical Physics* **157**, 174117 (2022), https://pubs.aip.org/aip/jcp/article-pdf/doi/10.1063/5.0114688/16553899/174117.1_online.pdf.
- ¹²H. R. Grimsley, S. E. Economou, E. Barnes, and N. J. Mayhall, “An adaptive variational algorithm for exact molecular simulations on a quantum computer,” *Nature Communications* **10** (2019), 10.1038/s41467-019-10988-2.
- ¹³D. Mondal, D. Halder, S. Halder, and R. Maitra, “Development of a compact Ansatz via operator commutativity screening: Digital quantum simulation of molecular systems,” *The Journal of Chemical Physics*

- 159**, 014105 (2023), <https://pubs.aip.org/aip/jcp/article-pdf/doi/10.1063/5.0153182/18032301/014105.1.5.0153182.pdf>.
- ¹⁴M. Metcalf, N. P. Bauman, K. Kowalski, and W. A. de Jong, "Resource-efficient chemistry on quantum computers with the variational quantum eigensolver and the double unitary coupled-cluster approach," *Journal of Chemical Theory and Computation* **16**, 6165–6175 (2020), PMID: 32915568, <https://doi.org/10.1021/acs.jctc.0c00421>.
- ¹⁵N. P. Bauman and K. Kowalski, "Coupled cluster downfolding theory: towards universal many-body algorithms for dimensionality reduction of composite quantum systems in chemistry and materials science," *Materials Theory* **6**, 17 (2022).
- ¹⁶D. A. Fedorov, Y. Alexeev, S. K. Gray, and M. Otten, "Unitary Selective Coupled-Cluster Method," *Quantum* **6**, 703 (2022).
- ¹⁷M. Haidar, M. J. Rančić, Y. Maday, and J.-P. Piquemal, "Extension of the trotterized unitary coupled cluster to triple excitations," *The Journal of Physical Chemistry A* **127**, 3543–3550 (2023), PMID: 37039518, <https://doi.org/10.1021/acs.jpca.3c01753>.
- ¹⁸Y. Fan, C. Cao, X. Xu, Z. Li, D. Lv, and M.-H. Yung, "Circuit-depth reduction of unitary-coupled-cluster ansatz by energy sorting," (2023), arXiv:2106.15210 [quant-ph].
- ¹⁹S. Halder, A. Dey, C. Shrikhande, and R. Maitra, "Machine learning assisted construction of a shallow depth dynamic ansatz for noisy quantum hardware," *Chem. Sci.*, – (2024).
- ²⁰I. Lindgren, J. Morrison, I. Lindgren, and J. Morrison, "First-order perturbation for closed-shell atoms," *Atomic Many-Body Theory*, 212–223 (1986).
- ²¹I. Shavitt and R. J. Bartlett, "Many-body methods in chemistry and physics: Mbpt and coupled-cluster theory," *Cambridge Molecular Science* (2009), 10.1017/CBO9780511596834.
- ²²J. Romero, R. Babbush, J. R. McClean, C. Hempel, P. J. Love, and A. Aspuru-Guzik, "Strategies for quantum computing molecular energies using the unitary coupled cluster ansatz," *Quantum Science and Technology* **4**, 014008 (2018).
- ²³D. Halder, S. Halder, D. Mondal, C. Patra, A. Chakraborty, and R. Maitra, "Corrections beyond coupled cluster singles and doubles through selected generalized rank-two operators: digital quantum simulation of strongly correlated systems," *Journal of Chemical Sciences* **135**, 41 (2023).
- ²⁴Z. W. Windom, D. Claudino, and R. J. Bartlett, "A new "gold standard": perturbative triples corrections in unitary coupled cluster theory and prospects for quantum computing," (2024), arXiv:2401.06036 [physics.chem-ph].
- ²⁵F. A. Evangelista, G. K.-L. Chan, and G. E. Scuseria, "Exact parameterization of fermionic wave functions via unitary coupled cluster theory," *The Journal of Chemical Physics* **151**, 244112 (2019), https://pubs.aip.org/aip/jcp/article-pdf/doi/10.1063/1.5133059/16659468/244112.1_online.pdf.
- ²⁶T. Q. N. developers and contributors, "Qiskit nature 0.6.0," (2023).
- ²⁷Q. Sun, T. C. Berkelbach, N. S. Blunt, G. H. Booth, S. Guo, Z. Li, J. Liu, J. D. McClain, E. R. Sayfutyarova, S. Sharma, S. Wouters, and G. K.-L. Chan, "Pyscf: the python-based simulations of chemistry framework," *WIREs Computational Molecular Science* **8**, e1340 (2018), <https://wires.onlinelibrary.wiley.com/doi/pdf/10.1002/wcms.1340>.
- ²⁸W. J. Hehre, R. F. Stewart, and J. A. Pople, "Self-consistent molecular-orbital methods. i. use of gaussian expansions of Slater-type atomic orbitals," *The Journal of Chemical Physics* **51**, 2657–2664 (1969), <https://doi.org/10.1063/1.1672392>.
- ²⁹J. T. Seeley, M. J. Richard, and P. J. Love, "The bravyi-kitaev transformation for quantum computation of electronic structure," *The Journal of Chemical Physics* **137**, 224109 (2012), <https://doi.org/10.1063/1.4768229>.
- ³⁰R. H. Byrd, P. Lu, J. Nocedal, and C. Zhu, "A limited memory algorithm for bound constrained optimization," *SIAM Journal on Scientific Computing* **16**, 1190–1208 (1995), <https://doi.org/10.1137/0916069>.
- ³¹Y. S. Yordanov, D. R. M. Arvidsson-Shukur, and C. H. W. Barnes, "Efficient quantum circuits for quantum computational chemistry," *Phys. Rev. A* **102**, 062612 (2020).
- ³²Y. S. Yordanov, V. Armaos, C. H. W. Barnes, and D. R. M. Arvidsson-Shukur, "Qubit-excitation-based adaptive variational quantum eigensolver," *Communications Physics* **4**, 228 (2021).
- ³³I. Magoulas and F. A. Evangelista, "Cnot-efficient circuits for arbitrary rank many-body fermionic and qubit excitations," *Journal of Chemical Theory and Computation* **19**, 822–836 (2023), PMID: 36656643, <https://doi.org/10.1021/acs.jctc.2c01016>.
- ³⁴S. Halder, C. Shrikhande, and R. Maitra, "Development of zero-noise extrapolated projective quantum algorithm for accurate evaluation of molecular energetics in noisy quantum devices," *The Journal of Chemical Physics* **159**, 114115 (2023), <https://pubs.aip.org/aip/jcp/article-pdf/doi/10.1063/5.0166433/18129554/114115.1.5.0166433.pdf>.
- ³⁵K. Kowalski and N. P. Bauman, "Quantum flow algorithms for simulating many-body systems on quantum computers," *Phys. Rev. Lett.* **131**, 200601 (2023).